

The Wall Effect of the Sample Position Well in the Measurement of Fission Fragments

Huaiyong Bai, Haoyu Jiang, Yi Lu, Zengqi Cui, Jinxiang Chen, Guohui Zhang*

State Key Laboratory of Nuclear Physics and Technology, Institute of Heavy Ion Physics, Peking University, Beijing 100871, China

Yu.M. Gledenov, M.V. Sedysheva
Frank Laboratory of Neutron Physics, JINR, Dubna 141980, Russia

G. Khuukhenkhoo
Nuclear Research Centre, National University of Mongolia, Ulaanbaatar, Mongolia

*Corresponding author: guohuizhang@pku.edu.cn

Abstract: The twin-gridded ionization chamber is widely used in the measurement of charged particles from neutron induced reactions. In many cases, a ^{238}U sample is mounted in the sample position well at the common cathode to monitor the neutron flux. In the experiments, some of the fission fragments with emission angle near 90° will collide with the inner wall of the sample position well, leading the measured pulse height to be lower, i.e. the wall effect of the sample position well. The wall effect of the sample position well is affected by the working gas pressure and the dimension of the ^{238}U sample and the sample position well. In the present work, simulations and experiments are performed to quantify the influence of the working gas pressure and the dimension of the ^{238}U sample and the sample position well on the wall effect of the sample position well in the measurement of ^{238}U fission fragments.

Key words: ionization chamber; wall effect; sample position well; fission fragments

1. Introduction

The measurement of neutron induced fission fragments is highly concerned in radiation measurement for the following two aspects. Firstly, the standard cross sections are useful in monitoring the neutron flux [1,2], i.e. $^{235}\text{U}(n, f)$ and $^{238}\text{U}(n, f)$. Secondly, the research on neutron induced fission fragments is important in nuclear physics and applications [3,4]. Gridded ionization chambers are widely used in measuring the neutron induced fission fragments because of its high detection efficiency, γ insensitive and radiation resistant, et al. [4–7]. In many cases, the prepared fissile samples are mounted in a sample position well to simultaneously measure the emitted fission fragments in both the forward and the backward directions, or to replace the samples conveniently [8,9]. In these situations, the fission fragment may collide with the inner wall of the sample position well and only a part of its kinetic energy can be deposited in the working gas. Thus, the measured pulse amplitude of the corresponding event will be lower [7]. This is the wall effect of the sample position well for fission fragments which is simplified as the wall effect below.

The wall effect can decrease the proportion of the fission events above the measurement threshold, which means that the determined detection efficiency will be overestimated if the wall effect is ignored. Because the wall effect is more significant for fission fragments with larger emission angle, especially with emission angles near 90° , the measured angular distribution will be incorrect. Therefore, the wall effect for neutron induced fission fragments is important.

In the present work, the wall effect for neutron induced fission fragments is studied using Monte Carlo simulation reliability of which is validated by the experiment. In section 2, the measurement of the energy spectrum of neutron induced fission fragments is illustrated, and the Monte Carlo simulation of the energy spectrum is introduced. In section 3, the factors of the wall effect is studied using the Monte Carlo simulation. Finally, the conclusions are drawn in section 4.

2. The experiment and the simulation

2.1 The experiment

The sketch of the experimental setup, including a neutron source and a gridded ionization chamber, is presented in Fig. 1. The 5.5 MeV neutrons were generated using a deuterium gas target bombarded by the deuteron beam. The pressure of the gas target was ~ 0.30 MPa and the length was ~ 2.0 cm. The deuteron beam ~ 2.5 μA was accelerated by the 4.5 MV Van de Graff accelerator of Peking University.

The gridded ionization chamber, details of which were presented in Ref. [9], was used as the detector of the charged particles. The separation of the cathode-grid was ~ 61.0 mm and that of the grid-anode was ~ 15.0 mm. The working gas was Kr + 2.7% CO₂ mixtures 0.052 MPa in pressure. The grid shielding inefficiency was about 0.017 [7, 10]. The data acquisition system (DAQS), with which the cathode-anode coincident signals can be recorded, was introduced in Ref. [11].

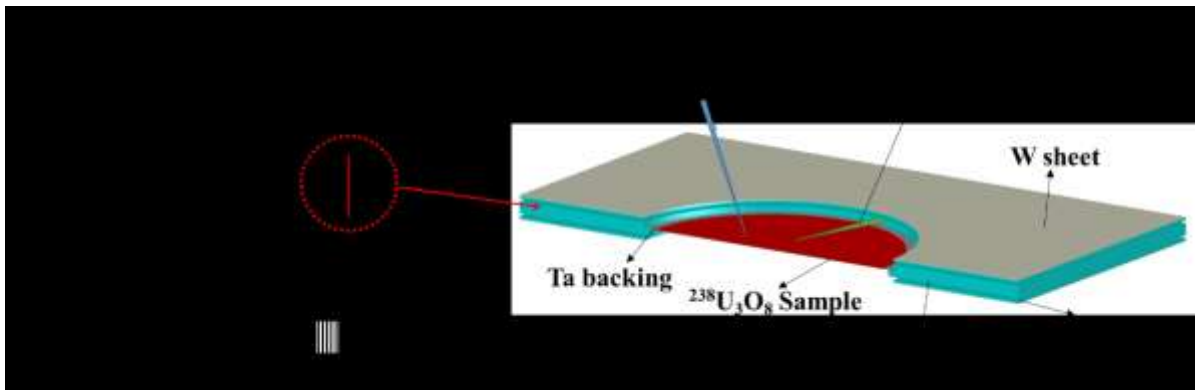


Fig. 1. The sketch of the experimental setup.

At the cathode of the gridded ionization chamber, there was a sample changer with five sample position wells. Back-to-back samples can be mounted in each of them as shown in Fig. 1. The sample changer was made of aluminum. Except for the measured sample, the samples mounted in the other sample position wells were covered by aluminum plates at both sides [7]. To decrease the background of neutron induced charged particles, the whole cathode was covered by tungsten sheets at both sides. The thicknesses of the tungsten sheets were 0.1 mm. The radii of the sample position wells were ~ 24.0 mm and the depths were ~ 2.0 mm [7].

A highly enriched $^{238}\text{U}_3\text{O}_8$ sample ($> 99.999\%$) was used in the experiment [12]. This $^{238}\text{U}_3\text{O}_8$ sample was prepared using painting method with 22.5 mm in radius. The thickness of the $^{238}\text{U}_3\text{O}_8$ sample was about 605 $\mu\text{g}/\text{cm}^2$ with non-uniformity ~ 1.00 [13]. The sample was mounted in one of the five sample position wells as shown in Fig. 1. The backing was a tantalum sheet 0.1 mm in thickness.

The measured energy spectrum of the neutron induced fission fragments is illustrated in Fig. 2. The energy of the higher energy peak is ~ 90 MeV according to the simulation

introduced below. Since the position of the peak is not very clear, a little deviation of the determined energy is expected.

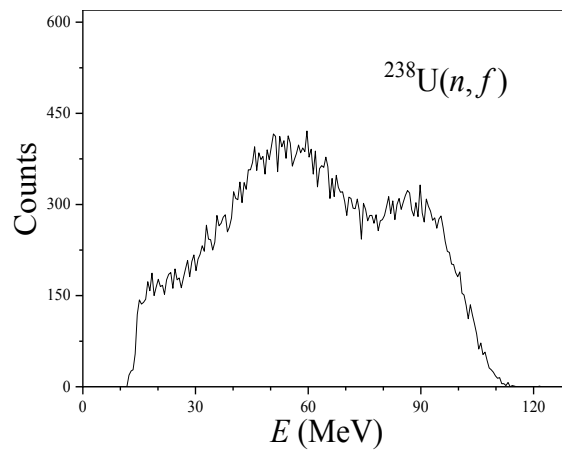


Fig. 2. The measured energy spectrum of the neutron induced fission fragments.

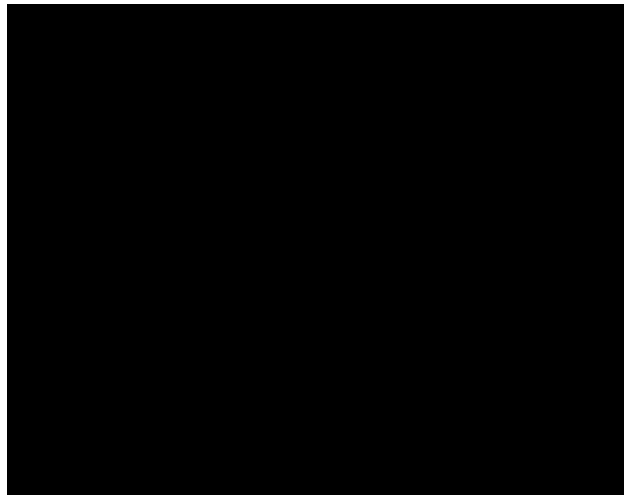


Fig. 3. The flowchart of the Monte Carlo simulation.

2.2 The simulation

The simulation is based on Monte Carlo method which is similar to that introduced in Ref. [13]. According to Ref. [13], the effect of the scattering of the fission fragment can be ignored without inducing noticeable deviations, and only those fission fragments with orientations toward the working gas need to be tracked.

The flowchart of the simulation is presented in Fig. 3. In the simulation, A fission fragment (atomic number, mass and yield) is sampled from the cumulative fission products yields taken from ENDF/B-VII.1 library [14,15]. The fission fragments with yields which are lower than 1/1000 of the highest one are ignored in the simulation to improve the efficiency of the simulation. The energy of the fission fragment E_f is determined by its mass using the results of Ref. [4]. As the energies of different fragments with the same mass may be different, a random number E_w is sampled from normal distribution $N(0, \sigma_w)$ where σ_w is the width of the energy as a function of the mass published by Birgersson [4]. The initial energy of the fission fragment in the simulation is $E_f + E_w$. The (x, y) position of the fission fragment is

sampled randomly with the restriction of $x^2 + y^2 \leq r^2$ ($r = 22.5$ mm which is the radius of the $^{238}\text{U}_3\text{O}_8$ sample). The thickness h of the $^{238}\text{U}_3\text{O}_8$ sample at (x, y) equals to the average thickness multiplying w which is a weight factor sampled from the normal distribution $N(1.00, 1.00)$ because the non-uniformity of the $^{238}\text{U}_3\text{O}_8$ sample is 1.00 [13]. If the sampled w is negative or bigger than 10, a new w will be sampled to make sure that the thickness of the $^{238}\text{U}_3\text{O}_8$ sample is reasonable. The z position of the fission fragment is randomly sampled from $[0, h]$. The orientation of the fission fragment is sampled from isotropic distribution [15]. Since the probability of the fission reaction is proportional to the thickness, the weight of the fission fragment is wy where y is the yield of the fission fragment taken from ENDF/B-VII.1 library [15].

The fission fragment moves forward step by step. In each step the energy loss is set to be 0.05 MeV with step length decided by the stopping power calculated using SRIM-2013 Code [16]. If the fission fragment entrances the working gas, the energy ΔE deposited in each step will increase the anode signal amplitude of the gridded ionization chamber by ΔA calculated using

$$\Delta A = \Delta E \left(1 - \eta \frac{d}{D_{cg}} \right), \quad (1)$$

where η is the grid shielding inefficiency, d is the distance from the cathode to the spot where the energy ΔE is deposited, and D_{cg} is the separation of the cathode-grid. It should be pointed out that the stopping powers of the fission fragments with the same atomic number are assumed to be the same, and this will not induce noticeable deviations as explained in Ref. [13].

The fission fragment will not stop unless its energy is degraded below 0.05 MeV or it collides with the inner wall of the sample position well. After it stops, the fission fragment will be counted. The simulated results of 10^5 fission fragments are shown in Fig. 4. In the simulated energy spectrum of the neutron induced fission fragments, the valley near 0 MeV is caused by the gap between the inner wall of the sample position well and the edge of the $^{238}\text{U}_3\text{O}_8$ sample, and the counts at 0 MeV is caused by the self-absorption effect.

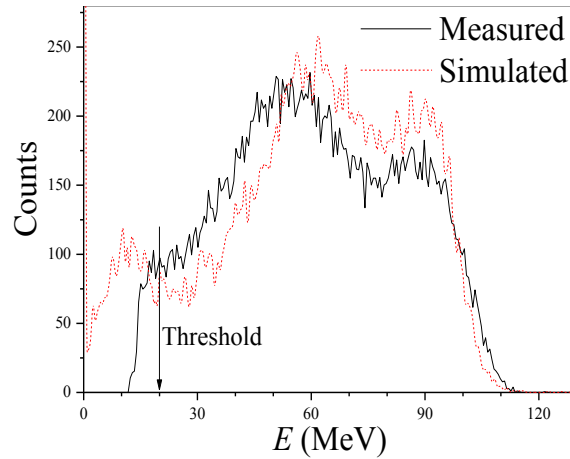


Fig. 4. The energy spectra of neutron induced fission fragments. The solid line and the dashed line are the measured and simulated ones, separately.

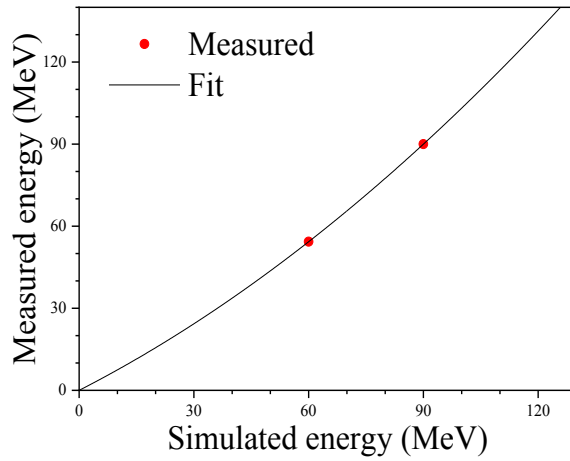


Fig. 5. The relationship between the measured energy and the simulated energy of the neutron induced fission fragments.

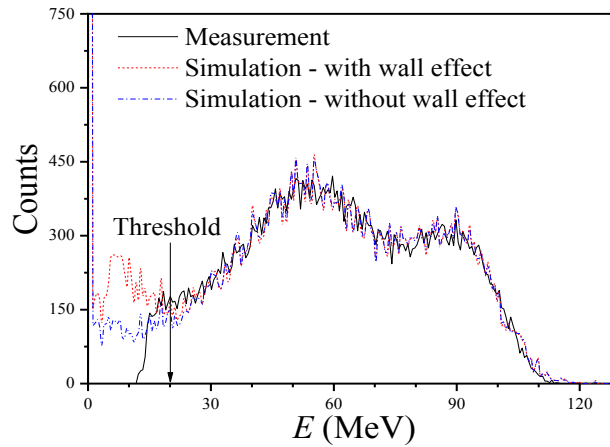


Fig. 6. The energy spectra of the neutron induced fission fragments. The solid line is the measured one. The dashed line and the dash dotted line are the simulated ones with and without considering the wall effect, respectively.

Since the Pulse Height Defect (PHD) effect is not considered in the simulation, the energy of the measured lower energy peak is lower than that of the simulated one. Actually the energy of the measured higher energy peak should also be lower than that of the simulated one due to the PHD effect. Because the PHD effect is generally more significant for heavy fission fragments which correspond to the lower energy peak [17], the energy of the measured lower energy peak is still lower than that of the simulated one even if the energy of the measured higher energy peak is assumed to be equal to that of the simulated one [13]. The PHD effect has not been measured by us, and there is no related data which can be used according to our knowledge. The simulated energy of the neutron induced fission fragment is adjusted using [13]

$$E_M = aE_S + bE_S^2, \quad (2)$$

where E_M and E_S are the energies of the two peaks of the measured and the simulated energy spectra, separately, a and b are the fitting parameters. Because the PHD effect is more noticeable for heavy fission fragments [8], the increase of the measured energy is slower in lower energy region as shown in Fig. 5. After the energy scaling, the simulated energy spectra

accords well with the measured one as presented in Fig. 6, and this proves that the simulated result is reliable.

As shown in Fig. 6, the difference between the simulations with and without considering the wall effect is obvious in low energy regions. If the wall effect is ignored, the detection efficiency above the measurement threshold will be overestimated by 5% which proves the significance of the wall effect.

3. Discussions about the wall effect

To illustrate the wall effect more clearly, simulation, in which the self-absorption and the PHD effects are ignored to exclude their interferences, is performed. In this case, only the wall effect can affect the energy deposition in the working gas and the result indicates that ~14% of the fission fragments will be affected by the wall effect. As shown in Fig. 7, the tail below 50 MeV is caused by the wall effect.

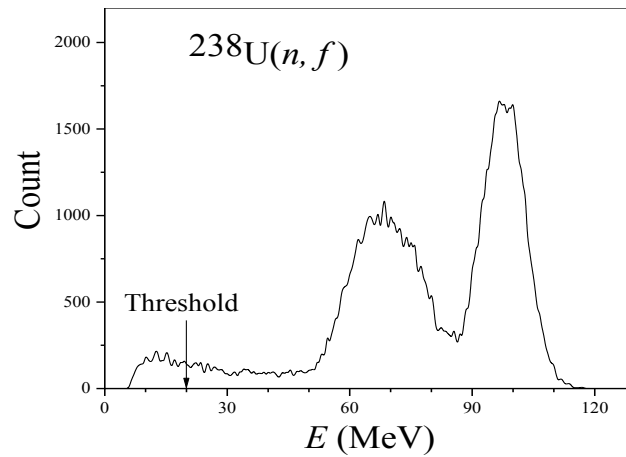


Fig. 7. The simulated energy spectrum of the neutron induced fission fragments.

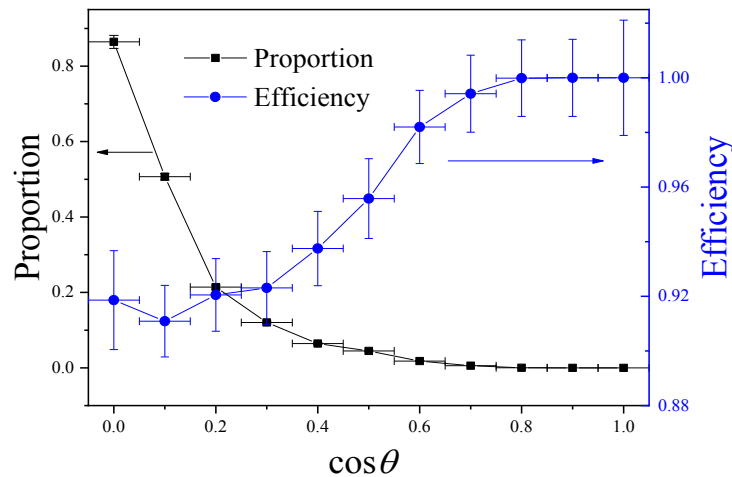


Fig. 8. The proportion of the fission fragments with the wall effect (square) and the detection efficiency of the fission fragments (circle) as functions of the cosine of the emission angle.

3.1 The wall effect for fission fragments with different emission angles

If the fission fragment collides with the inner wall of the sample position well, only a part of its energy will be deposited in the working gas. Thus, the signal amplitude of the fission fragments may be decreased to below the measurement threshold, so that the corresponding detection efficiency may be decreased. In Fig. 8, the proportion of the fission

fragments with the wall effect and the detection efficiency of the fission fragments as functions of the cosine of the emission angle are presented. If the emission angle is bigger than 45° ($\cos\theta < 0.7$) the wall effect will be noticeable. As shown in Fig. 8, the bigger of the emission angle, the higher proportion of the fission fragments with the wall effect and the lower detection efficiency of those fission fragments are. This indicates that if the wall effect is ignored, the detection efficiency will be overestimated and the measured angular distribution will be incorrect.

3.2 Factors which influence the wall effect

The wall effect can be influenced by some factors which will affect the collisions between the fission fragments and the inner wall of the sample position well. In general, the lower pressure of the working gas (the longer range of the fission fragment), the bigger radius of the $^{238}\text{U}_3\text{O}_8$ sample, the smaller radius and the deeper depth of the sample position well, the stronger of the wall effect is. To illustrate the influences of these factors, simulations are performed and the results are illustrated in Fig. 9.

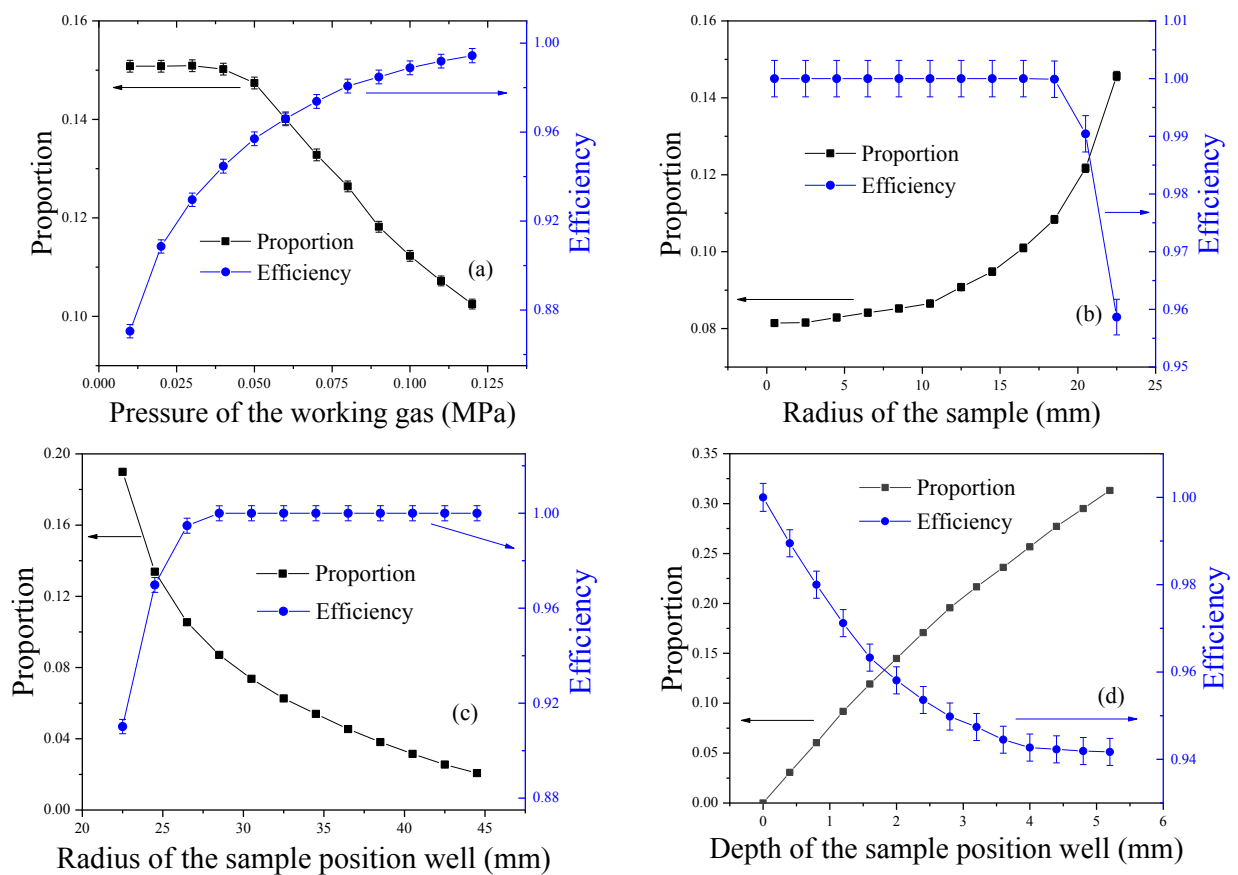


Fig. 9. The proportion of the fission fragments with the wall effect (square), and the detection efficiency of the fission fragments (circle). (a), the influence of the working gas pressure (the radius of the sample is 22.5 mm, the radius and the depth of the sample position well are 24.0 and 2.0 mm, separately); (b), the influence of the radius of the $^{238}\text{U}_3\text{O}_8$ sample (the working gas pressure is 0.052 MPa, the radius and the depth of the sample position well are 24.0 and 2.0 mm, respectively); (c), the influence of the radius of the sample position well (the working gas pressure is 0.052 MPa, the radius of the sample and the depth of the sample position well are 22.5 and 2.0 mm, separately); and (d), the influence of the depth of the sample position well (the working gas pressure is 0.052 MPa, the radii of the sample and the sample position well are 22.5 and 24.0 mm, respectively).

As shown in Fig. 9(a), the proportion of the fission fragments with the wall effect decreases with the increase of the working gas pressure because more fission fragments will be stopped before they reach the inner wall of the sample position well. As a result, the detection efficiency will be higher since the wall effect is weaker.

In Fig. 9(b), the proportion of the fission fragments with the wall effect increase with the increase of the radius of the sample, because the fission fragments generated near the inner wall of the sample position well are more likely to collide with the inner wall of the sample position well. Although the proportion of the fission fragments is higher and higher, the detection efficiency of the fission fragments will not change if the radius of the sample is smaller than 16.5 mm. This is because the separation between the sample's edge and the inner wall of the sample position well is big enough so that the deposited energies of the fission fragments are high enough to surpass the measurement threshold.

Contrary to the situation in Fig. 9(b), the proportion of the fission fragments with the wall effect decreases with the increase of the radius of the sample position well as shown in Fig. 9(c). Thus, the detection efficiency of the fission fragment increase with the increase of the radius of the sample position well. If the radius of the sample position well is bigger than 28.5 mm, all the fission fragments will be detected although some fission fragments are still affected by the wall effect. This is because before the fission fragment reaches the inner wall of the sample position well, the deposited energy will be high enough to surpass the measurement threshold.

Fig. 9(d) shows that the proportion of the fission fragments with the wall effect increases with the increase of the depth of the sample position well, because the fission fragment with smaller emission angle may collide with the inner wall of the sample position well if the sample position well is deeper. The detection efficiency of the fission fragments thus decreases with the increase of the depth of the sample position well.

4. Conclusions

In the present work, the wall effect of the fission fragments is illustrated using Monte Carlo simulation. According to the simulation, the proportion of the fission fragments with the wall effect can be as big as 14%, and the wall effect is more significant for the fission fragment with larger emission angle. Because the detected energy of the fission fragments with the wall effect may degraded below the measurement threshold, the determined detection efficiency of the fission fragments will be overestimated if the wall effect is ignored.

Since the conditions of the experiments may be various, the significance of the wall effect should be different. In general, the wall effect will be more significant if the working gas pressure is lower (the range of the fission fragment is longer), or the radius of the sample is bigger, or the radius of the sample position well is smaller, or the sample position well is deeper.

ACKNOWLEDGEMENTS

The authors are indebted to the operation crew of the 4.5 MV Van de Graff accelerator of Peking University. The present work is financially supported by the National Natural Science Foundation of China (Nos. 11475007 and 11775006), Science and Technology on Nuclear Data Laboratory and China Nuclear Data Center.

References

1. A.D. Carlson, V.G. Pronyaev, D.L. Smith et al., Nuclear Data Sheets 110 (2009): 3215–3324.
2. Neutron Cross-section Standards, 2006, <https://www-nds.iaea.org/standards/>.
3. F. Vives, F.J. Hambsch, H. Bax et al., Nuclear Physics **662** (1) (2000):63–92.
4. E. Birgersson, A. Oberstedt, S. Oberstedt et al., Nuclear Physics A **817** (2009): 1–34.
5. G. Zhang, Y.M. Gledenov, G. Khuukhenkhuu et al., Physical Review C **82** (2010): 054619.
6. G.A. Tutin, I.V. Ryzhov, V.P. Eismont et al., Nuclear Instruments and Methods in Physics Research A **457** (2001): 646–652.
7. H. Bai, Z. Wang, L. Zhang et al., Applied Radiation and Isotopes **125** (2017): 34–41.
8. D.L. Duke, F. Tovesson, A.B. Laptev et al., Physical Review C **94** (2016): 054604.
9. Z. Chen, X. Zhang, Y. Chen et al., Nuclear Physics Review **16** (1) (1999): 31–36.
10. O. Bunemann, T.E. Cranshaw, J.A. Harvey, Canadian Journal of Research A **27** (5) (1949): 191–206.
11. G. Zhang, H. Wu, J. Zhang et al., Eur. Phys. J. A **43**, 1 (2010).
12. G. Zhang, X. Liu, Z. Gao et al., Applied Radiation and Isotopes **70** (2012): 888–892.
13. H. Bai, H. Jiang, Z. Cui et al., Determination of the amount of ^{238}U target nuclei and simulation of the neutron induced fission fragment energy spectrum, submitted to Applied Radiation and Isotopes.
14. C. Jammes, P. Filliatre, P. Loiseau et al., Nuclear Instruments and Methods in Physics Research A **681** (2012): 101–109.
15. ENDF/B-VII.1, 2011, U.S. Evaluated Nuclear Data Library, <https://www-nds.iaea.org/exfor/endl.htm>.
16. J.F. Ziegler, 2013, SRIM -2013, <http://www.srim.org/#SRIM>.
17. D.L. Duke, F. Tovesson, A.B. Laptev et al., Physical Review C **94** (2016): 054604.